Postprint of: Malikan, M, Eremeyev, VA., Effect of surface on the flexomagnetic response of ferroic composite nanostructures; nonlinear bending analysis, COMPOSITE STRUCTURES (2021), DOI: 10.1016/j.compstruct.2021.114179

Effect of surface on the flexomagnetic response of ferroic composite nanostructures; nonlinear bending analysis

Mohammad Malikan[1], Victor A. Eremeyev[1,2,3]*

[1] Department of Mechanics of Materials and Structures, Gdansk University of Technology, 80-233 Gdansk, Poland

[2] Research and Education Center "Materials" Don State Technical University, Gagarina sq., 1, 344000 Rostov on Don, Russia

[3] DICAAR, Università degli Studi di Cagliari, Via Marengo, 2, 09123, Cagliari, Italy

*Corresponding author:
Email: victor.eremeev@pg.edu.pl, eremeyev.victor@gmail.com

Abstract

Our analysis incorporates the geometrically nonlinear bending of the Euler-Bernoulli ferromagnetic nanobeam accounting for a size-dependent model through assuming surface effects. In the framework of the flexomagnetic phenomenon, the large deflections are investigated referring to von-Kármán nonlinearity. Employing the nonlocal effects of stress coupled to the gradient of strain generates a scale-dependent Hookean stress-strain scheme related to the small scale. Taking into account the supports of the nanobeam in two cases,

that is, totally fixed and hinged, the deformations are predicted. A constant static lateral load is postulated uniformly along the length of the beam, which forces the deformation. As the analysis is based on the one-dimensional media, the electrodes are embedded so that they give off a transverse magnetic field creating a longitudinal force. The newly developed mathematical model is computed by means of the differential quadrature method together with the Newton-Raphson technique. The computational section discusses and reveals the numerical results in detail for the characteristics and parameters involved in the design of beam-like magnetic nanosensors. As shown later, the conducted research presents that there is a strong linkage between the surface effect and the flexomagneticity behavior of the bulk.

Keywords: Flexomagnetic; Euler-Bernoulli beam; Surface effects; Nonlinear bending; Nonlocal strain gradient theory; Differential quadrature method

List of symbols

σ_{xx}	Stress component	u	Axial displacement of the mid-plane
ε_{xx}	Strain component	w	Transverse displacement of the mid-plane
C_{11}	Elasticity modulus	q_{31}	Component of the third-order *piezomagnetic* tensor
ν	Poisson's ratio	g_{31}	Component of the sixth-order gradient elasticity tensor
m	Mode number	f_{31}	Component of fourth-order flexomagnetic tensor
z	Thickness coordinate	a_{33}	Component of the second-order *magnetic permeability* tensor
I_z	Area moment of inertia	N^{Mag}	In-plane axial magnetic force
L	Length of the beam	A	Area of cross-section of the beam
ψ	Magnetic potential		
b	Width of the beam		
h	Thickness of the beam		

1 Introduction

Flexomagnetic coupling is between magnetic polarization and strain gradient or reversely,

elastic strain and magnetic field gradient. The perception of the flexomagnetic effect dates back to not-so-distant years, which can be a pervasive influence for all structures including symmetrical and nonsymmetrical crystals. However, studies of flexomagneticity in solids are rare in bulk samples due to the small amount of this effect. With the development of nanoscale technology, interest in flexomagnetic has renewed; because the large strain gradient is often manifested at the nanoscale, which leads to a strong flexomagnetic effect. One of the attractive applications of piezomagnetic is the extraction of energy from the mechanical vibrations of the environment in order to power micro-and nanodevices. However, piezomagnetic is limited to specific materials and is strongly influenced by temperature, which does not exist in flexomagnetic. This feature can be considered as a higher-order effect than piezomagneticity. The gradient size effect shows that the importance of the flexomagnetic effect in micro-and nanosystems is comparable to piezomagnetic and even beyond. In addition, flexomagnetic, unlike piezomagnetic, is found in any material with any symmetry. This means that compared to piezomagneticity, which is inefficient and invalid in materials with central symmetry, the effects of flexomagnetic are present in all biological materials and systems. These features have led to a growing interest and research in flexomagnetic in the last decade. As expected, in the future the effect of piezomagnetic on nanomotors and nano memory has important applications, the flexomagnetic effect may also play such an important role in the construction of these devices [1-9].

As a brief physical explanation of this effect, it can be mentioned that by bending a crystal, the atomic layers are stretched inside it, and it is clear that the outermost layer will have the most tension. A magnetic field can be created into the crystal due to the movement of ions as a result of tension differences between the different layers. In other words, bending some materials creates a magnetic field, which is called flexomagnetism.

The effect of flexomagnetic in nanoscale should be considered and evaluated in light of several reasons, including [1-9]: a- Flexomagneticity is a pervasive property of any structural symmetry compared to piezomagnetic, and therefore expands the choice of materials that can be used for sensors and electro-magneto-mechanical actuators. b- Reduced dimensions lead to a larger strain gradient, meaning that the strain difference at smaller distances results in the larger strain gradient. The small scale is introduced in nanotechnology and therefore leads to an increase in the effect of flexomagnetism, which at the nanoscale can compete with piezomagnetism. c- A number of experiments have reported strong flexomagnetic coupling constants that are several times higher than theoretical estimates.

Utterly different properties can be revealed for body surfaces from those dedicated to the interior [10] on account of unalike environmental conditions. At very small sizes, the importance of surface property can be pivotally considerable owing to the high surface-to-volume ratio. In spite of the significance of surface effects at the mesoscale, it can be responsible as a size-dependent property. Gurtin and Murdoch [11, 12] posed a mathematical schema in terms of a continuum elasticity framework involving effects of the surface, where the surface was assumed as a virtual layer with zero thickness concerning a mathematical layer, in which the membrane has dissimilar material features and characteristics and underlying the layer as an entirely bonding with the bulk.

By an exact look at the literature, the extensity can be found in studies of surface effects phenomena with electro-magneto-elastic coupling [13-18]. However, the study of the flexomagnetic effect does exist in none of them, and the need to examine it is quite obvious which merits an investigation between surface effect and flexomagneticity. Furthermore, mathematical studies on the impact of flexomagneticity on micro/nanostructures have been extended slowly hitherto [19-26]. Despite the attention to this issue in recent years,

flexomagnetism has still many questions, ambiguities, and unresolved issues. According to the literature, it was found and confirmed that the surface effects can strongly and directly affect the electro-magneto-elastic coupling in an electro-elastic nanomaterial. For this reason, we were persuaded to theoretically consider the surface effect on the flexomagneticity as a higher-order coupling effect in ferrite nanostructures. In this research, while re-introducing the flexomagnetic effect and the relations governing its static bending, theoretical discussions on the subject are presented considering the effect of the surface layer. Specifically, a theoretical explanation of the effect of the surface layer on the flexomagnetic effect is given and the reason for its importance in nanoscale systems is stated. Noted that the effects of surface residual stress are eliminated in this paper and the surface energy alone has been investigated. After explaining the physical model of the theory, the governing relations are solved using the numerical method of differential quadrature and specifically the Newton-Raphson method. Finally, the potential effects of the surface layer on the flexomagnetic effect are represented.

2 Mathematical Model

Regarding Fig. 1, the magnetic nanomaterial specimen in the form of a rectangular nanobeam with initial length L and height/thickness h is schematically discussed in an orthogonal coordinate system. The left-most end of the beam is postulated as the location of the rectangular coordinate system. Two flexible electrodes are covered and attached to the top and bottom transversal surfaces of the beam, which are connected to an ampere meter. These electrodes produce a lateral magnetic field.

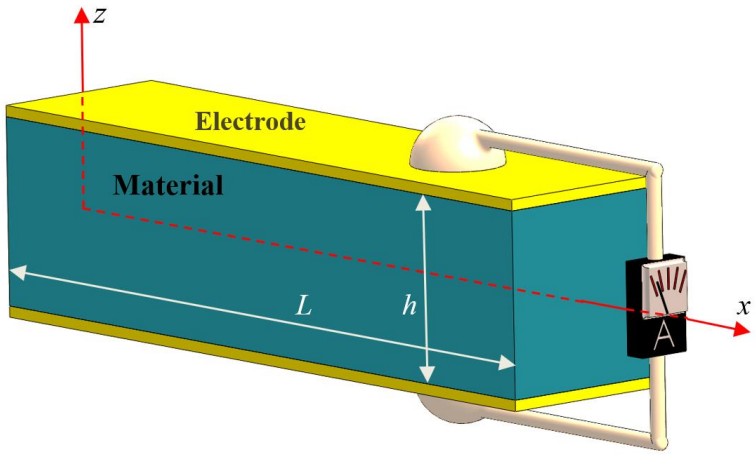

Fig. 1. A square magnetic material specimen connected to a magnetic system

The engineer's beam theory (Euler–Bernoulli beam) will here describe how the beam nodes move after deformations and displacements [23-26]

$$u_1(x,z) = u(x) - z\frac{dw(x)}{dx} \tag{1}$$

$$u_3(x,z) = w(x) \tag{2}$$

Basic constitutive equations of the present problem were also argued in the literature as [23-26],

$$\frac{dN_{xx}}{dx} = 0 \tag{3}$$

$$\frac{d^2M_{xx}}{dx^2} + \frac{d^2T_{xxz}}{dx^2} + N_{xx}^0\frac{d^2w}{dx^2} = 0 \tag{4}$$

The nonlocal strain gradient size-dependent model [27-36] has advantages in contrast to Eringen's nonlocal elasticity theory [37-40] and coupled stress/strain gradient approaches [41-47] which contain one length scale factor only. Thus, the nonlinear nonlocal strain gradient static elasticity bending model of flexoferroic beam-like magnetic nanomaterial involving flexomagnetic effect is made available by use of [48]

$$C_{11}A\left[\frac{d^2u}{dx^2}+\frac{d^2w}{dx^2}\frac{dw}{dx}-l^2\left(\frac{d^4u}{dx^4}+\frac{d^4w}{dx^4}\frac{dw}{dx}+3\frac{d^3w}{dx^3}\frac{d^2w}{dx^2}\right)\right]=0 \tag{5}$$

$$-g_{31}h\frac{d^4w}{dx^4}+q_{31}\psi\frac{d^2w}{dx^2}-p-\mu\left(-g_{31}h\frac{d^6w}{dx^6}+q_{31}\psi\frac{d^4w}{dx^4}-\frac{d^2p}{dx^2}\right)$$
$$-\mu C_{11}A\left[\frac{du}{dx}+\frac{1}{2}\left(\frac{dw}{dx}\right)^2\right]\frac{d^4w}{dx^4}+C_{11}A\mu l^2\left[\frac{d^3u}{dx^3}+\frac{d^3w}{dx^3}\frac{dw}{dx}+\left(\frac{d^2w}{dx^2}\right)^2\right]\frac{d^4w}{dx^4}$$
$$-\mu C_{11}A\left(\frac{d^2u}{dx^2}+\frac{dw}{dx}\frac{d^2w}{dx^2}\right)\frac{d^3w}{dx^3}+C_{11}A\mu l^2\left(\frac{d^4u}{dx^4}+3\frac{d^3w}{dx^3}\frac{d^2w}{dx^2}+\frac{dw}{dx}\frac{d^4w}{dx^4}\right)\frac{d^3w}{dx^3}$$
$$-\mu C_{11}A\left(\frac{d^4u}{dx^4}+\frac{dw}{dx}\frac{d^4w}{dx^4}+3\frac{d^3w}{dx^3}\frac{d^2w}{dx^2}\right)\frac{dw}{dx}+C_{11}A\left[\frac{du}{dx}+\frac{1}{2}\left(\frac{dw}{dx}\right)^2\right]\frac{d^2w}{dx^2}$$
$$+C_{11}A\mu l^2\left(\frac{d^6u}{dx^6}+\frac{dw}{dx}\frac{d^6w}{dx^6}+5\frac{d^5w}{dx^5}\frac{d^2w}{dx^2}+10\frac{d^4w}{dx^4}\frac{d^3w}{dx^3}\right)\frac{dw}{dx}$$
$$-C_{11}Al^2\left[\frac{d^3u}{dx^3}+\frac{d^3w}{dx^3}\frac{dw}{dx}+\left(\frac{d^2w}{dx^2}\right)^2\right]\frac{d^2w}{dx^2}+C_{11}A\left(\frac{d^2u}{dx^2}+\frac{dw}{dx}\frac{d^2w}{dx^2}\right)\frac{dw}{dx}$$
$$-I_z\left(C_{11}+\frac{q_{31}^2}{a_{33}}\right)\left(\frac{d^4w}{dx^4}-l^2\frac{d^6w}{dx^6}\right)-C_{11}Al^2\left(\frac{d^4u}{dx^4}+3\frac{d^3w}{dx^3}\frac{d^2w}{dx^2}+\frac{dw}{dx}\frac{d^4w}{dx^4}\right)\frac{dw}{dx}=0 \tag{6}$$

Along with the longitudinal direction, the surface effect is important. This issue can be mathematically modeled by the following one-dimensional relation [49],

$$\sigma^S=C_{11}^S\varepsilon_{11}^S \tag{7}$$

in which C_{11}^S denotes the surface elasticity modulus which the value may be found either based on experiments or atomic simulations [50, 51]. Noted that, in this paper, the upper index *S* introduces constants relate to the surface layer.

The effective axial and flexural rigidities showed by Eq. (7) can be calculated as [52-56],

$$C_{11}^{*}I_{z}^{*}=C_{11}\frac{bh^{3}}{12}+C_{11}^{S}\left(\frac{bh^{2}}{2}+\frac{h^{3}}{6}\right) \tag{8}$$

Moreover, the effective magnetic properties can be written as follows,

$$f_{11}^{*}=f_{11}+f_{11}^{S} \tag{9}$$

$$q_{31}^{*}=q_{31}+q_{31}^{S} \tag{10}$$

$$a_{33}^{*}=a_{33}+a_{33}^{S} \tag{11}$$

Accounts for the surface effect, the governing differential equations which define the large deflections of the magnetic beam-like nanomaterial can be conducted as,

$$C_{11}^{*}A^{*}\left[\frac{d^{2}u}{dx^{2}}+\frac{d^{2}w}{dx^{2}}\frac{dw}{dx}-l^{2}\left(\frac{d^{4}u}{dx^{4}}+\frac{d^{4}w}{dx^{4}}\frac{dw}{dx}+3\frac{d^{3}w}{dx^{3}}\frac{d^{2}w}{dx^{2}}\right)\right]=0 \tag{12}$$

$$-g_{31}^{*}h\frac{d^{4}w}{dx^{4}}+q_{31}^{*}\psi\frac{d^{2}w}{dx^{2}}-p-\mu\left(-g_{31}^{*}h\frac{d^{6}w}{dx^{6}}+q_{31}^{*}\psi\frac{d^{4}w}{dx^{4}}-\frac{d^{2}p}{dx^{2}}\right)$$
$$-\mu C_{11}^{*}A^{*}\left[\frac{du}{dx}+\frac{1}{2}\left(\frac{dw}{dx}\right)^{2}\right]\frac{d^{4}w}{dx^{4}}+C_{11}^{*}A^{*}\mu l^{2}\left[\frac{d^{3}u}{dx^{3}}+\frac{d^{3}w}{dx^{3}}\frac{dw}{dx}+\left(\frac{d^{2}w}{dx^{2}}\right)^{2}\right]\frac{d^{4}w}{dx^{4}}$$
$$-\mu C_{11}^{*}A^{*}\left(\frac{d^{2}u}{dx^{2}}+\frac{dw}{dx}\frac{d^{2}w}{dx^{2}}\right)\frac{d^{3}w}{dx^{3}}+C_{11}^{*}A^{*}\mu l^{2}\left(\frac{d^{4}u}{dx^{4}}+3\frac{d^{3}w}{dx^{3}}\frac{d^{2}w}{dx^{2}}+\frac{dw}{dx}\frac{d^{4}w}{dx^{4}}\right)\frac{d^{3}w}{dx^{3}}$$
$$-\mu C_{11}^{*}A^{*}\left(\frac{d^{4}u}{dx^{4}}+\frac{dw}{dx}\frac{d^{4}w}{dx^{4}}+3\frac{d^{3}w}{dx^{3}}\frac{d^{2}w}{dx^{2}}\right)\frac{dw}{dx}+C_{11}^{*}A^{*}\left[\frac{du}{dx}+\frac{1}{2}\left(\frac{dw}{dx}\right)^{2}\right]\frac{d^{2}w}{dx^{2}}$$
$$+C_{11}^{*}A^{*}\mu l^{2}\left(\frac{d^{6}u}{dx^{6}}+\frac{dw}{dx}\frac{d^{6}w}{dx^{6}}+5\frac{d^{5}w}{dx^{5}}\frac{d^{2}w}{dx^{2}}+10\frac{d^{4}w}{dx^{4}}\frac{d^{3}w}{dx^{3}}\right)\frac{dw}{dx}-C_{11}^{*}A^{*}l^{2}\times$$
$$\left[\frac{d^{3}u}{dx^{3}}+\frac{d^{3}w}{dx^{3}}\frac{dw}{dx}+\left(\frac{d^{2}w}{dx^{2}}\right)^{2}\right]\frac{d^{2}w}{dx^{2}}+C_{11}^{*}A^{*}\left(\frac{d^{2}u}{dx^{2}}+\frac{dw}{dx}\frac{d^{2}w}{dx^{2}}\right)\frac{dw}{dx}-I_{z}^{*}\left(C_{11}^{*}+\frac{q_{31}^{*2}}{a_{33}^{*}}\right)$$
$$\times\left(\frac{d^{4}w}{dx^{4}}-l^{2}\frac{d^{6}w}{dx^{6}}\right)-C_{11}^{*}A^{*}l^{2}\left(\frac{d^{4}u}{dx^{4}}+3\frac{d^{3}w}{dx^{3}}\frac{d^{2}w}{dx^{2}}+\frac{dw}{dx}\frac{d^{4}w}{dx^{4}}\right)\frac{dw}{dx}=0 \tag{13}$$

3 Solution of equations

Let us apply an accurate and convenient numerical solution method, namely the differential quadrature method (DQM), to transfer the nonlinear differential equations displayed by Eqs. (12, 13) into algebraic ones to advance the solution [57-66]. In comparison with other numerical techniques employed to solve complicated differential equations, such as finite difference, finite element, and dynamic relaxation, the differential quadrature technique provides low computational cost and simple procedure.

For a one-dimensional problem, the first-order derivative of variables is carried out as

$$\frac{du}{dx}\left(x_i\right)=\sum_{k=1}^{N}a_{ik}^{x}U\left(x_k\right),\quad i=1,2,...,N \tag{14a}$$

$$\frac{dw}{dx}\left(x_i\right)=\sum_{k=1}^{N}a_{ik}^{x}W\left(x_k\right),\quad i=1,2,...,N \tag{14b}$$

where the number of grid points along the axial direction is depicted by N. Moreover, a^{x} is expressed as follows,

$$\begin{cases} a_{ij}^{x}=\dfrac{R\left(x_i\right)}{\left(x_i-x_j\right)R\left(x_j\right)} & \text{for } i\neq j \\ a_{ii}^{x}=-\displaystyle\sum_{j=1,\neq i}^{N}a_{ij}^{x}, & i,j=1,2,...,N \end{cases} \tag{15}$$

in which

$$R\left(x_i\right)=\prod_{j=1,\neq i}^{N}\left(x_i-x_j\right) \tag{16}$$

In addition, higher-order derivatives can be written as

$$\frac{d^{(n)}u}{dx^{(n)}}\left(x_i\right)=\sum_{k=1}^{N}C_{ik}^{(n)}U\left(x_k\right) \tag{17a}$$

$$\frac{d^{(n)}w}{dx^{(n)}}(x_i)=\sum_{k=1}^{N}C_{ik}^{(n)}W(x_k) \tag{17b}$$

where $C^{(n)}$ shows a weighting equation which can be defined as follows,

$$C^{(1)}=a^x \tag{18}$$

$$\begin{cases} C_{ij}^{(n)}=n\left[a_{ij}^{x}C_{ii}^{(n-1)}-\dfrac{C_{ij}^{(n-1)}}{x_i-x_j}\right] \quad \text{for } i\neq j \\ C_{ii}^{(n)}=-\sum_{j=1,\neq i}^{N}C_{ij}^{(n)}, \quad i,j=1,2,...,N \end{cases} \tag{19}$$

Another issue that needs to be mentioned is how to mesh the beam. Different methods have been proposed for distributing nodes in the mesh network. The simplest type of meshing is the uniform distribution of nodes on the surface of the beam with equal distances. This type of meshing, although simple, is often less accurate. A high efficient mesh point can be obtained by embedding Chebyshev– Gauss–Lobatto relation as,

$$x_i=\frac{L}{2}\left(1-\cos\left(\frac{i-1}{N-1}\pi\right)\right) \;\; ; \;\; i=1,2,...,N \tag{20}$$

In fact, this type of meshing leads to more stability of the equations and the speed of convergence of the results.

Implementation of the DQM presents Eqs. (12, 13) in the following scheme,

$$\begin{aligned} &C_{11}^{*}A^{*}\left[\sum_{k=1}^{N}C_{ik}^{(2)}U(x_k)+\sum_{k=1}^{N}C_{ik}^{(2)}W(x_k)\times\sum_{k=1}^{N}C_{ik}^{(1)}W(x_k)-l^2\times\left(\sum_{k=1}^{N}C_{ik}^{(4)}U(x_k)\right.\right. \\ &\left.\left.+\sum_{k=1}^{N}C_{ik}^{(4)}W(x_k)\times\sum_{k=1}^{N}C_{ik}^{(1)}W(x_k)+3\times\sum_{k=1}^{N}C_{ik}^{(3)}W(x_k)\times\sum_{k=1}^{N}C_{ik}^{(2)}W(x_k)\right)\right]=0 \end{aligned} \tag{21}$$

$$-g_{31}^{*}h\sum_{k=1}^{N}C_{ik}^{(4)}W\left(x_k\right)+q_{31}^{*}\psi\sum_{k=1}^{N}C_{ik}^{(2)}W\left(x_k\right)-p-\mu\left(-g_{31}^{*}h\sum_{k=1}^{N}C_{ik}^{(6)}W\left(x_k\right)+q_{31}^{*}\psi\sum_{k=1}^{N}C_{ik}^{(4)}W\left(x_k\right)\right)+$$

$$\mu\frac{d^2p}{dx^2}-\mu C_{11}^{*}A^{*}\left[\sum_{k=1}^{N}C_{ik}^{(1)}U\left(x_k\right)+\frac{1}{2}\left(\sum_{k=1}^{N}C_{ik}^{(1)}W\left(x_k\right)\right)^2\right]\times\sum_{k=1}^{N}C_{ik}^{(4)}W\left(x_k\right)+C_{11}^{*}A^{*}\mu l^2\left[\sum_{k=1}^{N}C_{ik}^{(3)}U\left(x_k\right)\right.$$

$$\left.+\sum_{k=1}^{N}C_{ik}^{(3)}W\left(x_k\right)\times\sum_{k=1}^{N}C_{ik}^{(1)}W\left(x_k\right)+\left(\sum_{k=1}^{N}C_{ik}^{(2)}W\left(x_k\right)\right)^2\right]\times\sum_{k=1}^{N}C_{ik}^{(4)}W\left(x_k\right)-\mu C_{11}^{*}A^{*}\left(\sum_{k=1}^{N}C_{ik}^{(2)}U\left(x_k\right)+\right.$$

$$\left.\sum_{k=1}^{N}C_{ik}^{(1)}W\left(x_k\right)\times\sum_{k=1}^{N}C_{ik}^{(2)}W\left(x_k\right)\right)\times\sum_{k=1}^{N}C_{ik}^{(3)}W\left(x_k\right)+C_{11}^{*}A^{*}\mu l^2\left(\sum_{k=1}^{N}C_{ik}^{(4)}U\left(x_k\right)+3\sum_{k=1}^{N}C_{ik}^{(3)}W\left(x_k\right)\times\right.$$

$$\left.\sum_{k=1}^{N}C_{ik}^{(2)}W\left(x_k\right)+\sum_{k=1}^{N}C_{ik}^{(1)}W\left(x_k\right)\times\sum_{k=1}^{N}C_{ik}^{(4)}W\left(x_k\right)\right)\times\sum_{k=1}^{N}C_{ik}^{(3)}W\left(x_k\right)-\mu C_{11}^{*}A^{*}\left(\sum_{k=1}^{N}C_{ik}^{(4)}U\left(x_k\right)+\right.$$

$$\left.\sum_{k=1}^{N}C_{ik}^{(1)}W\left(x_k\right)\times\sum_{k=1}^{N}C_{ik}^{(4)}W\left(x_k\right)+3\times\sum_{k=1}^{N}C_{ik}^{(3)}W\left(x_k\right)\times\sum_{k=1}^{N}C_{ik}^{(2)}W\left(x_k\right)\right)\times\sum_{k=1}^{N}C_{ik}^{(1)}W\left(x_k\right)+C_{11}^{*}A^{*}\times$$

$$\left[\sum_{k=1}^{N}C_{ik}^{(1)}U\left(x_k\right)+\frac{1}{2}\left(\sum_{k=1}^{N}C_{ik}^{(1)}W\left(x_k\right)\right)^2\right]\times\sum_{k=1}^{N}C_{ik}^{(2)}W\left(x_k\right)+C_{11}^{*}A^{*}\mu l^2\left(\sum_{k=1}^{N}C_{ik}^{(6)}U\left(x_k\right)+\sum_{k=1}^{N}C_{ik}^{(1)}W\left(x_k\right)\right.$$

$$\left.\times\sum_{k=1}^{N}C_{ik}^{(6)}W\left(x_k\right)+5\times\sum_{k=1}^{N}C_{ik}^{(5)}W\left(x_k\right)\times\sum_{k=1}^{N}C_{ik}^{(2)}W\left(x_k\right)+10\times\sum_{k=1}^{N}C_{ik}^{(4)}W\left(x_k\right)\times\sum_{k=1}^{N}C_{ik}^{(3)}W\left(x_k\right)\right)$$

$$\times\sum_{k=1}^{N}C_{ik}^{(1)}W\left(x_k\right)-C_{11}^{*}A^{*}l^2\times\left[\sum_{k=1}^{N}C_{ik}^{(3)}U\left(x_k\right)+\sum_{k=1}^{N}C_{ik}^{(3)}W\left(x_k\right)\times\sum_{k=1}^{N}C_{ik}^{(1)}W\left(x_k\right)+\left(\sum_{k=1}^{N}C_{ik}^{(2)}W\left(x_k\right)\right)^2\right]$$

$$\times\sum_{k=1}^{N}C_{ik}^{(2)}W\left(x_k\right)+C_{11}^{*}A^{*}\times\left(\sum_{k=1}^{N}C_{ik}^{(2)}U\left(x_k\right)+\sum_{k=1}^{N}C_{ik}^{(1)}W\left(x_k\right)\times\sum_{k=1}^{N}C_{ik}^{(2)}W\left(x_k\right)\right)\times\sum_{k=1}^{N}C_{ik}^{(1)}W\left(x_k\right)$$

$$-I_z^{*}\left(C_{11}^{*}+\frac{q_{31}^{*2}}{a_{33}^{*}}\right)\left(\sum_{k=1}^{N}C_{ik}^{(4)}W\left(x_k\right)-l^2\times\sum_{k=1}^{N}C_{ik}^{(6)}W\left(x_k\right)\right)-C_{11}^{*}A^{*}l^2\left(\sum_{k=1}^{N}C_{ik}^{(4)}U\left(x_k\right)+\sum_{k=1}^{N}C_{ik}^{(3)}W\left(x_k\right)\right.$$

$$\left.\times\sum_{k=1}^{N}C_{ik}^{(2)}W\left(x_k\right)+\sum_{k=1}^{N}C_{ik}^{(1)}W\left(x_k\right)\times\sum_{k=1}^{N}C_{ik}^{(4)}W\left(x_k\right)\right)\times\sum_{k=1}^{N}C_{ik}^{(1)}W\left(x_k\right)=0 \tag{22}$$

To complete the formulation, Eqs. (21, 22) are merged with the boundary conditions. These end conditions are exerted as follows,

Clamped (C): $U=W=0,\ M_x\neq 0\ \ :\ x=0,L$

Simply-supported (S): $U = W = M_x = 0 \quad : \quad x = 0, L$

Then, by inserting the introduced end conditions in Eqs. (21, 22), nonlinear algebraic matrix equations can be obtained.

The accuracy and convergence rate of the Newton-Raphson (NR) technique is quite high, leading to performing it on the current problem [67, 68]. In this approach, there should be primary guesses (X_0) whose amounts directly regulate the convergence rate. The first loop can be written as

$$X_1 = X_0 - J^{-1} \times A \tag{23}$$

in which *A* exhibits a *N*×1 matrix, *J* shows Jacobian that is a matrix of *N*×*N*.

$$J(i, j) = \frac{\partial e_i}{\partial x_j} \quad i, j = 1, ..., N \tag{24}$$

$$A(i,1) = e_i(X_0) \quad i = 1, ..., N \tag{25}$$

where *e* is dedicated for the nonlinear equilibrium equations. In a point of fact, Eq. (23) should be in an iterative form as

$$X_{n+1} = X_n - J^{-1} \times A \tag{26}$$

in which the iteration number *n* determines the convergence speed. The desired accuracy can be obtained based on a few iterations. As a consequence, Eq. (26) results in values of displacements along the *x* and *z* axes in which the deflections are related to the transverse axis.

4 Solution method validation

The method used to solve the nonlinear equations should be checked prior to the parametric study in order to assess its efficiency. Based on Tables 1 and 2, some results are tabulated which are reported from a finite element commercial software (FECS) and present study for

linear and nonlinear deflections of an isotropic local beam alongside simple and clamped supports. It is borne to keep it in mind that the convergence rate of the present solution method is N=9. To achieve large deflections, the chosen load is much bigger than that of the first comparison. The validation criterion is the length-to-thickness ratio, which is selected in a range from a thick beam up to a thin one.

The observation of these two tabulated examples says that in the case of large deflections the agreement is further passable particularly in terms of thinner beams. Of course, it should be logical as the present work used thin beam theory without involving shear deformations and, on the other side, FECS has the advantage of using shear deformations. More importantly, FECS considers large displacements in three axes, but the present formulation examines nonlinearity in the transverse axis respecting the von-Kármán theorem. Furthermore, the present mathematical model is based on the one-dimensional analysis; however, FECS is regarding three-dimensional problems. Regardless of these, FECS's outcomes vary due to lots of options in the solution, such as type of element, number of elements, and size. Consequently, a full matching among the results is not reasonable and the difference percentages ($Diff\% = \frac{|FECS - DQM|}{DQM} \times 100$) can be desirable. However, to give some information regarding FECS used here, it can be said that a high-quality standard Tetrahedral element with an average element size of 0.226h was practiced.

Table 1. Providing small deflections for a square macro beam (E=210GPa, h=10mm, p=100N/m, CC).

L/h	Linear deflections (mm)		
	FECS	Present (DQM)	Diff%
5	0.000272	0.000198	37.37%
10	0.001648	0.001585	3.97%

15	0.005243	0.005348	1.96%
20	0.012173	0.012680	3.99%
25	0.023553	0.024765	4.89%
30	0.040499	0.042790	5.35%
35	0.064131	0.067956	5.62%
40	0.095561	0.101440	5.79%
45	0.135907	0.144432	5.90%
50	0.186285	0.198126	5.97%

Table 2. Providing large deflections for a square macro beam (E=210GPa, h=10mm, p=0.5kN/m, CC).

L/h	Nonlinear deflections (mm)		
	FECS	Present (DQM)	Diff%
5	0.001362	0.000990	37.57%
10	0.008242	0.007924	4.01%
15	0.026218	0.026744	1.96%
20	0.060869	0.063371	3.94%
25	0.117767	0.123616	4.73%
30	0.202465	0.212890	4.89%
35	0.320469	0.335536	4.49%
40	0.477106	0.493667	3.35%
45	0.677421	0.685871	1.23%
50	0.925881	0.906756	2.10%

In order to more prove the validity of the present nonlinear NR algorithm, a nonlinear force-displacement diagram in comparison with FECS is provided in what follows. It is observed that our model which is based on the classical beam theory excluding shear deformations can be used while deflections are less than equal to 20 percent of thickness. More than this value of deflection, a shear deformation model is so vital to be used.

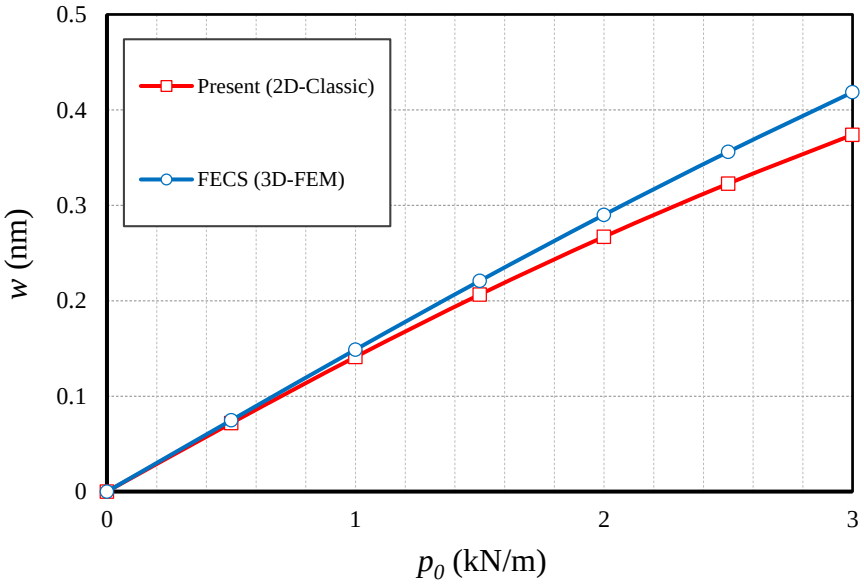

Fig. 2. Force-displacement diagram for the present model in comparison with FECS (L/h=10, h=1mm, CC)

5 Practical examples

The most fundamental concept in terms of nanoscale problems consists of establishing nanosize effects by formulating between continuum mechanics and nonlocal and also strain gradient approaches proposed theoretically. The concept of nonlocality expands and indicates interaction between atoms based on Eringen's postulations. It is discussed that stress at a point/atom under consideration relates not only to strain at that point but all atoms' strains in that media. This is mathematically meaningful by the Laplace operator which computes an average of a quantity in a planar domain. In addition to this, one can measure the large strain gradient of atoms by the use of well-known strain gradient elasticity models given by literature. These properties arrive from the bulk of a nanostructure. Another effective factor implies a nanostructure can behave differently against a macroscale and that this operator can be the effects of the exterior surface. Of course, surface effects happen on a macroscale though, this is eminent and more explicit on a small scale because of the large ratio of surface to volume.

As a matter of fact, [10-12] showed that the surface of materials reacts differently from bulk.

The focus of this section is to surface effects on the flexomagnetic behavior of the cobalt iron oxide as a ferromagnetic material with the structural properties assigned in Table 3 [69-72] and three categories, that is, a piezo-flexomagnetic (PFM) actuator, piezomagnetic (PM) and an ordinary nanobeam (NB).

Table 3. Employed structural properties

Bulk ($CoFe_2O_4$)	Surface layer
C_{11}=286GPa	C_{11}^S=35.3 N/m
f_{31}=10^{-9} N/A	f_{31}^S=10^{-9} N/A
q_{31}=580.3 N/A.m	q_{31}^S=3.4 N/A.m
a_{33}=1.57×10^{-4} N/A^2	a_{33}^S=1.4×10^{-4} H/m

In the first study of the correlation between flexomagnetic and surface effects, Figs. 3a and 3b are drawn with changes in nonlocal and strain gradient length scale (SGLS) coefficients. The aim here is that the surface layer affects the flexomagnetic behavior at smaller or larger values of these two small-scale parameters. In the first figure, which relies on the nonlocal parameter, it can be clearly seen that as we move towards the selection of larger values for the nonlocal parameter, the nonlocal parameter is effective in highlighting the flexomagnetic effect and it can increase the flexomagnetic response of the material even in the attendance of the surface effect. This result cannot be seen in Fig. 3b, and in fact, the boundary conditions have a direct effect on this achievement. Since the purpose of this study is to investigate the relationship between surface effect and flexomagnetic response, we will not interpret the results of the surface layer on the mechanics of the nanostructure. For example, the effect of the surface layer has led to a reduction in deflections and, as a result, greater stiffness of the material, which has been thoroughly discussed in the research background. Other results considered according to

these two figures show a growth in the flexomagnetic effect while the surface effect is not examined. This is because, as mentioned before, the effect of the surface leads to the stiffness of the material and as a result, deduces the deflections. As the deflections decrease, the flexomagnetic effect will be less important. In fact, if the nanostructure under study has inestimable surface effects, the flexomagnetic effect on that material will be larger.

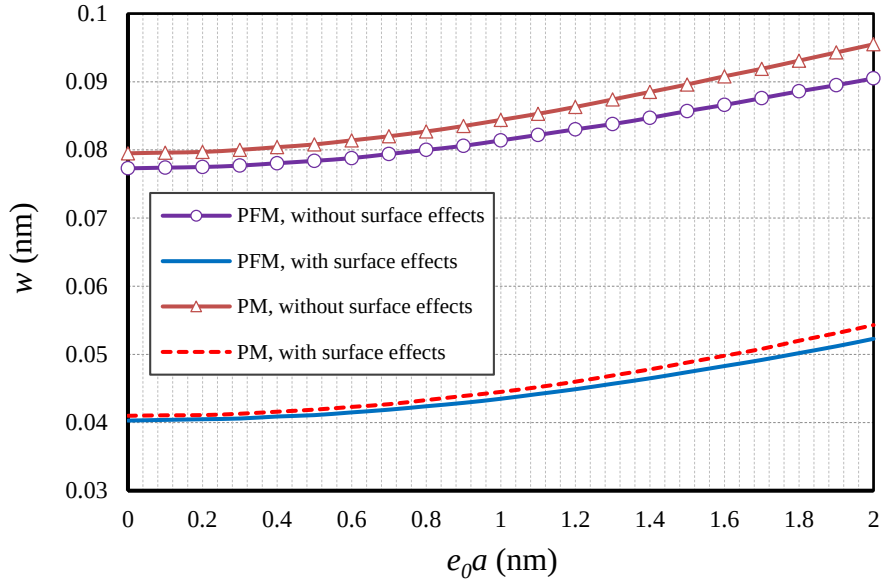

Fig. 3a. Nonlocal parameter vs. deflections for beams with and without surface effects (Ψ=1 mA, L/h=10, p_0=0.1 N/m, l=1 nm, CC)

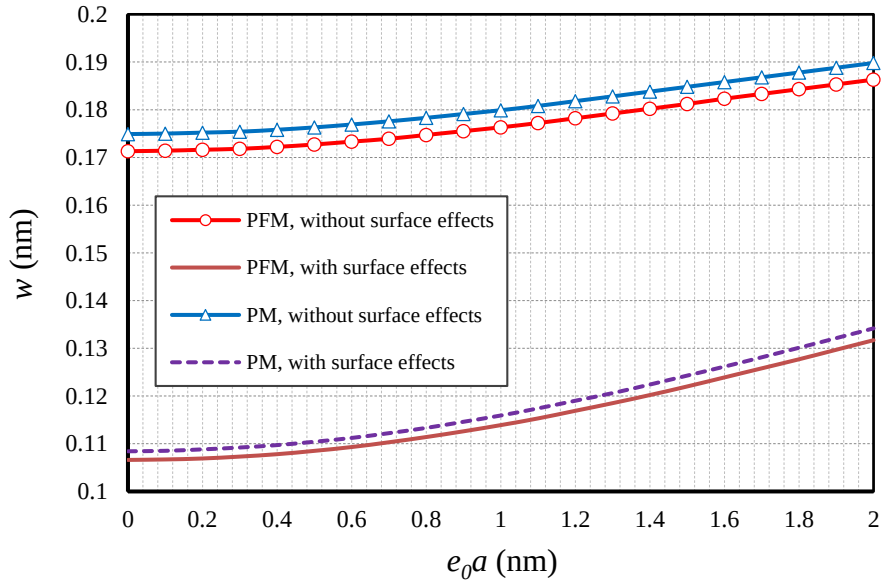

Fig. 3b. Nonlocal parameter vs. deflections for beams with and without surface effects (Ψ=1 mA, L/h=10, p_0=0.05 N/m, l=1 nm, SS)

In this section, by presenting Figs. 4a and 4b, there will be a similar study of Figs. 3a and 3b, with the difference that here the changes of the SGLS are evaluated. Since in the previous figures we have come to the conclusion that in larger values of the nonlocal parameter, despite the surface effect, the flexomagnetic effect becomes more dominant. This was because increasing the nonlocal parameter reduced the stiffness of the material, resulting in a larger strain gradient. Since the behavior of the SGLS parameter is the opposite of the nonlocal parameter, it means that its enhancement leads to an increase in the stiffness of the material and, as a rule, the flexomagnetic effect should be underestimated, which is simply shown in Fig. 4a. However, it cannot be found in Fig. 4b.

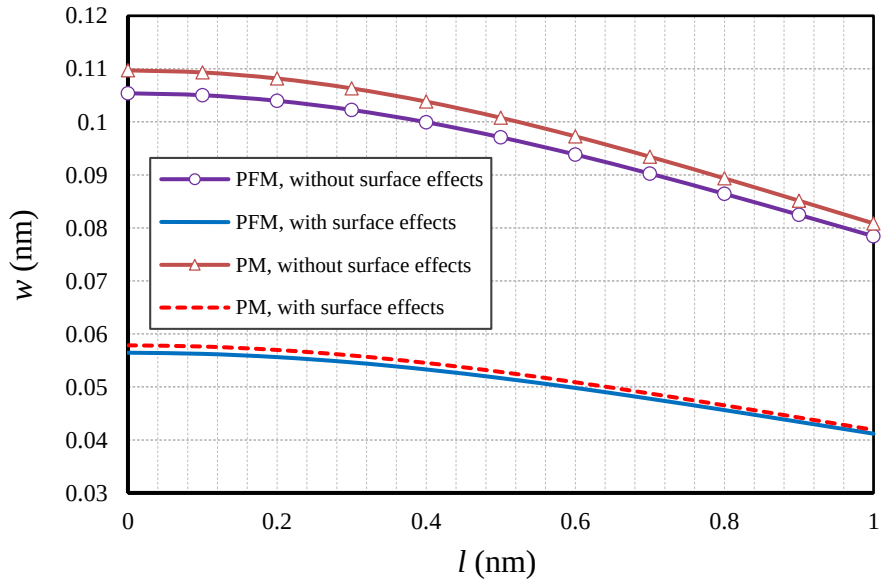

Fig. 4a. Nonlocal parameter vs. deflections for beams with and without surface effects (Ψ=1 mA, L/h=10, p_0=0.1 N/m, e_0a=0.5 nm, CC)

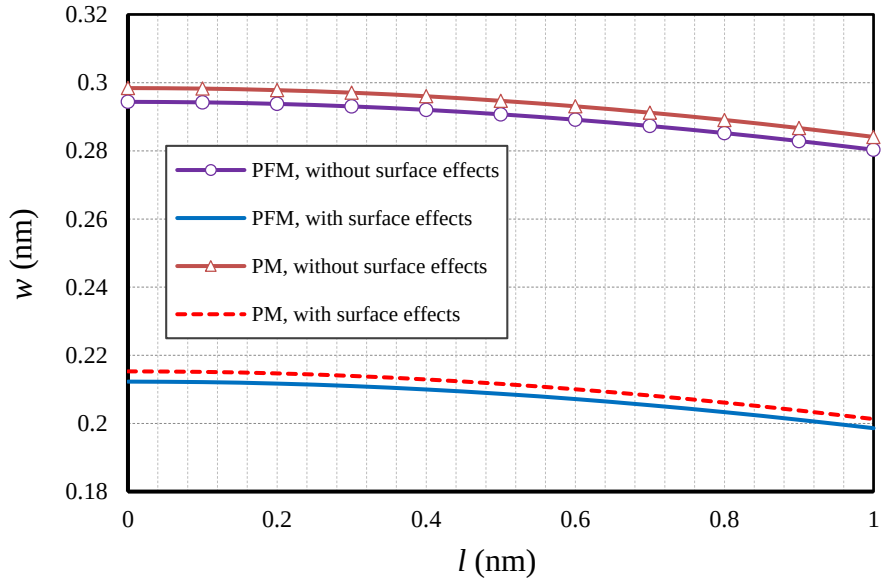

Fig. 4b. Nonlocal parameter vs. deflections for beams with and without surface effects (Ψ=1 mA, L/h=10, p_0=0.05 N/m, e_0a=0.5 nm, SS)

By preparing Figs. 5a and 5b, we consider the changes in transverse static load to find the effect of these changes on the connection between the surface layer and the flexomagnetic effect. As can be vividly seen, in the range of larger nonlinear deflections, the surface effect is more outstanding in particular when the loading is becoming greater in size. In the first figure, the difference between the results when the surface effect is examined compared with when it is omitted, the results are greater than those in the second figure. In fact, the first plot, which is prepared for the boundary condition of two clamped edges, shows that the larger the transverse load, the more substantial the surface effect, as well as its relationship to the flexomagnetic effect. However, if the two ends of the nanobeam use the hinge boundary condition, the differences will not increase significantly despite the larger static loads.

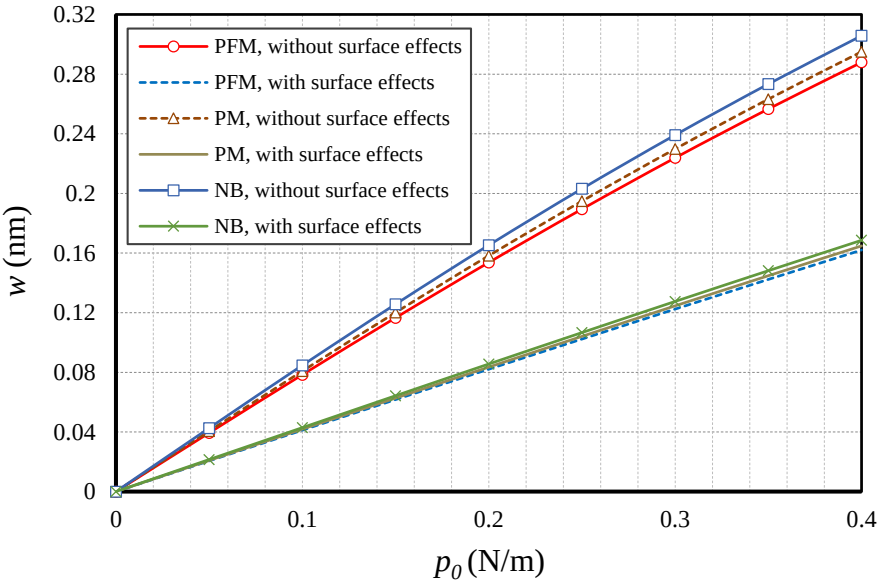

Fig. 5a. Static load vs. deflections for beams with and without surface effects (Ψ=1 mA, L/h=10, l=1 nm, e_0a=0.5 nm, CC)

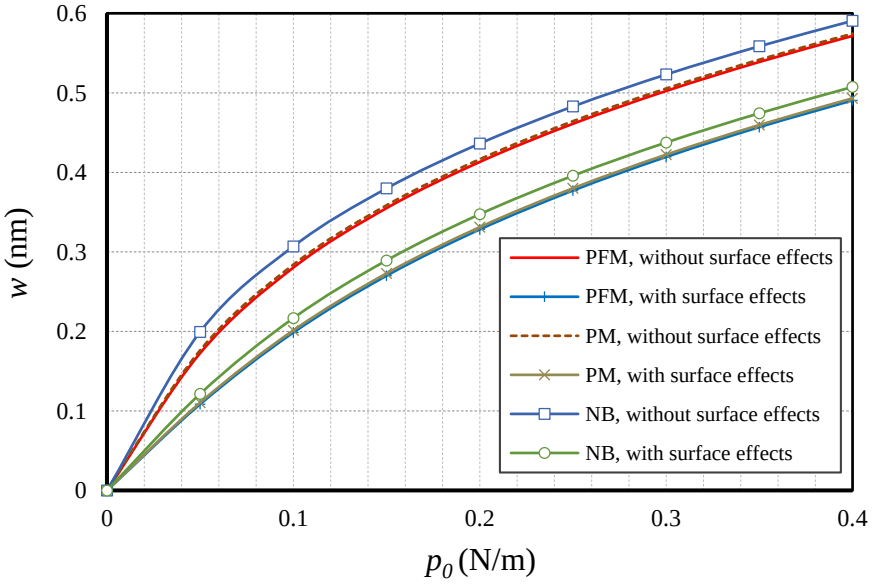

Fig. 5b. Static load vs. deflections for beams with and without surface effects (Ψ=1 mA, L/h=10, l=1 nm, e_0a=0.5 nm, SS)

At the end of the results section, by presenting two figures, Figs. 6a and 6b, which show the variations in the magnetic potential within the horizontal axis, we will evaluate any relationship between the surface effect and flexomagnetic at different values of the external magnetic

ampere. In the first figure, in the boundary conditions of two fixed edges, no serious result is obtained. However, by examining the second figure, which is related to the boundary conditions of two hinged edges, it can be seen that while the problem involves the surface effect, increasing the magnetic potential values leads to a very small reduction in the difference between results of PFM and PM. In fact, very little effect resulted from variation of the magnetic potential on the flexomagnetic effect can be observed. Nevertheless, as a general conclusion, it can be stated that changes in the magnetic potential do not have a noteworthy impact on the relationship between the flexomagnetic behavior of the bulk and the surface layer effect. On the other hand, by comparing the two figures, it can be concluded that the downward trajectory of the results is faster due to the increase of the magnetic potential in the hinge boundary conditions.

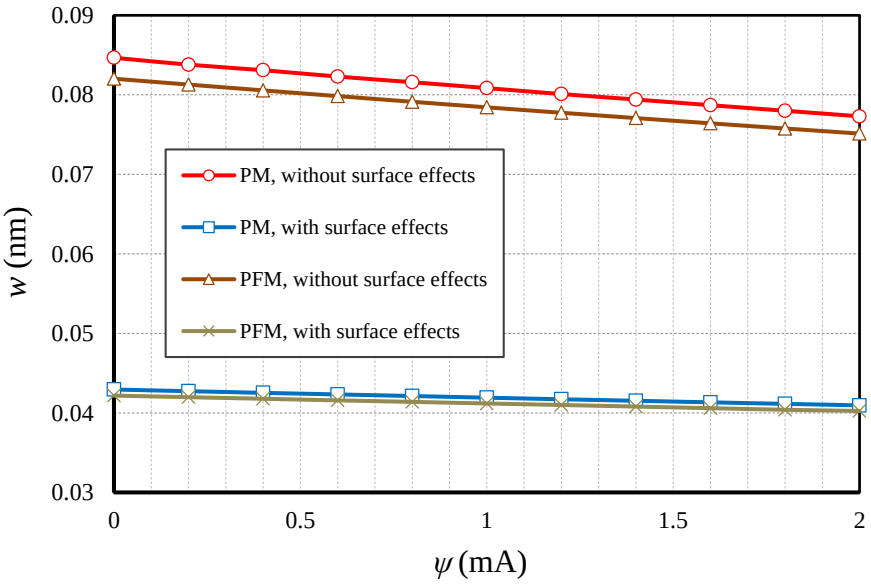

Fig. 6a. Magnetic ampere vs. deflections for beams with and without surface effects (L/h=10, l=1 nm, p_0=0.1 N/m, e_0a=0.5 nm, CC)

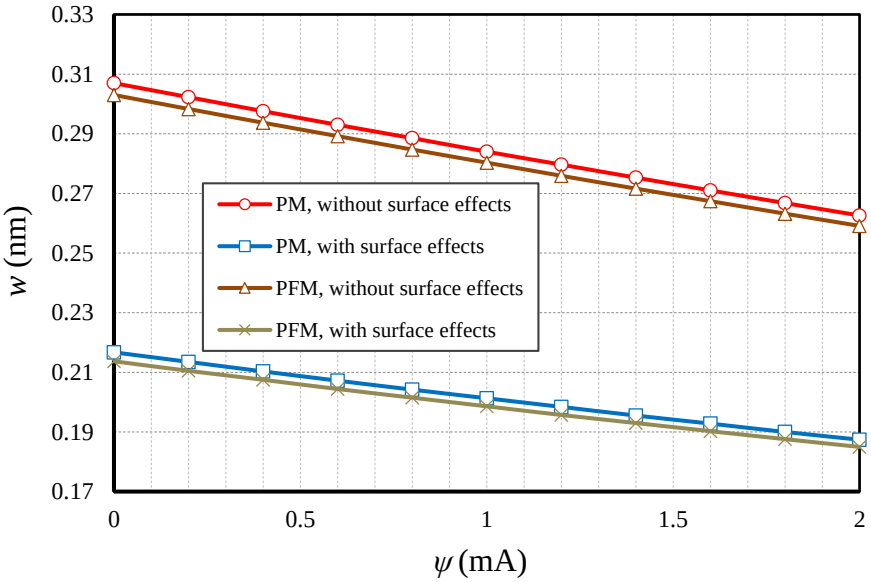

Fig. 6b. Magnetic ampere vs. deflections for beams with and without surface effects (L/h=10, l=1 nm, p_0=0.1 N/m, e_0a=0.5 nm, SS)

6 Conclusions

The work reported the effects of the surface layer on the various significance items included in a ferromagnetic structure for providing the flexomagnetic response. On the basis of the obtainable data of a flexoferroic material, an appropriate consideration was performed to predict the surface layer effect on the flexomagneticity. Euler-Bernoulli beam assumption was used to find out large deflections of clamped-clamped and pinned-pinned nanoscale beams. When the nonlocal strain gradient model is applied, it can generate the stress nonlocality and large gradient of atoms in the nanoscale. When the magnetic field gradient is applied, one can observe the converse flexomagnetic effect which was our case in this article. The contribution of the nonlinear von-Kármán strain aided us to mathematically model the problem. With the substitution of the differential quadrature method, which has been widely used and its precision has been entirely approved, the partial differential relations have been converted into algebraic equations. Thereafter, the algebraic relations were solved vis-à-vis the Newton-Raphson

technique to compute the large deflections. Further, investigations were warranted via a simple structure using a finite element commercial software before the results and discussion section. This study argued and demonstrated huge potential in affecting the flexomagnetic effect based on the surface layer. The suitable concluded remarks developed by this research will help the designers of small scale actuators and sensors, where some of them are indicated below,

- If the end conditions are selected as less flexible, and values of nonlocal parameter or SGLS are respectively, big and small enough, the surface layer can affect and develop a further flexomagnetic response.

- In general, the more dominant the surface effect, the stiffer the material, then the less important the flexomagnetic effect.

- The less flexible the end conditions, the remarkable the surface effect and its coherency with flexomagnetic effect if the lateral load is increasing.

- There was found no evidence to show that the relationship between the effect of the surface layer and the flexomagnetic influence can be affected by changes in values of the external magnetic ampere.

Acknowledgements

V.A.E acknowledges the support of the Government of the Russian Federation (contract No. 14.Z50.31.0046).

Data availability

The raw/processed data required to reproduce these findings cannot be shared at this time as the data also forms part of an ongoing study.

References

[1] W. Fahrner, Nanotechnology and Nanoelectronics, 1st ed.; Springer, Germany, 2005; pp. 269.

[2] P. Lukashev, R. F. Sabirianov, Flexomagnetic effect in frustrated triangular magnetic structures, Physical Review B 82 (2010) 094417.

[3] C. Pereira, A. M. Pereira, C. Fernandes, M. Rocha, R. Mendes, M. P. Fernández-García, A. Guedes, P. B. Tavares, J.-M. Grenèche, J. P. Araújo, and C. Freire, Superparamagnetic MFe_2O_4 (M = Fe, Co, Mn) Nanoparticles: Tuning the Particle Size and Magnetic Properties through a Novel One-Step Coprecipitation Route, Chemistry of Materials 24 (2012) 1496-1504.

[4] J. X. Zhang, R. J. Zeches, Q. He, Y. H. Chu, R. Ramesh, Nanoscale phase boundaries: a new twist to novel functionalities, Nanoscale 4 (2012) 6196-6204.

[5] H. Zhou, Y. Pei, D. Fang, Magnetic field tunable small-scale mechanical properties of nickel single crystals measured by nanoindentation technique, Scientific Reports 4 (2014) 1-6.

[6] S. Moosavi, S. Zakaria, C. H. Chia, S. Gan, N. A. Azahari, H. Kaco, Hydrothermal synthesis, magnetic properties and characterization of $CoFe_2O_4$ nanocrystals, Ceramics International 43 (2017) 7889-7894.

[7] E. A. Eliseev, A. N. Morozovska, V. V. Khist, V. Polinger, effective flexoelectric and flexomagnetic response of ferroics, In Recent Advances in Topological Ferroics and their Dynamics, Solid State Physics; Stamps, R. L., Schultheis, H.; Elsevier, Netherlands, 2019; Volume 70, pp. 237-289.

[8] A. F. Kabychenkov, F. V. Lisovskii, Flexomagnetic and flexoantiferromagnetic effects in centrosymmetric antiferromagnetic materials, Technical Physics, 64 (2019) 980-983.

[9] E. A. Eliseev, A. N. Morozovska, M. D. Glinchuk, R. Blinc, Spontaneous flexoelectric/flexomagnetic effect in nanoferroics, Physical Review B 79 (2009) 165433.

[10] J. E. Lennard-Jones, B. M. Dent, The change in lattice spacing at a crystal boundary.

Proceedings of the Royal Society A 121 (1928) 247-259.

[11] M. E. Gurtin, A. I. Murdoch, A continuum theory of elastic material surface, Archive for Rational Mechanics and Analysis 57 (1975) 291–323.

[12] M. E. Gurtin, A. I. Murdoch, Surface stress in solids, International Journal of Solids and Structures 14 (1978) 431–440.

[13] G.-L. Yu, H.-W. Zhang, Y.-X. Li, Modeling of magnetoelectric composite nano-cantilever beam with surface effect, Composite Structures 132 (2015) 65-74.

[14] Y. Yang, X.-F. Li, Bending and free vibration of a circular magnetoelectroelastic plate with surface effects, International Journal of Mechanical Sciences 157–158 (2019) 858-871.

[15] K. F. Wang, B. L. Wang, Nonlinear fracture mechanics analysis of nano-scale piezoelectric double cantilever beam specimens with surface effect, European Journal of Mechanics - A/Solids 56 (2016) 12-18.

[16] X. J. Xu, Z. C. Deng, K. Zhang, J.-M. Meng, Surface effects on the bending, buckling and free vibration analysis of magneto-electro-elastic beams, Acta Mechanica 227 (2016) 1557–1573.

[17] G. Sreenivasulu, S. K. Mandal, S. Bandekar, V. M. Petrov, and G. Srinivasan, Low-frequency and resonance magnetoelectric effects in piezoelectric and functionally stepped ferromagnetic layered composites, Physical Review B 84 (2011) 144426.

[18] C. Vazquez-Vazquez, M. A. Lopez-Quintela, M. C. Bujan-Nunez, J. Rivas, Finite size and surface effects on the magnetic properties of cobalt ferrite nanoparticles, Journal of Nanoparticle Research 13 (2011) 1663–1676.

[19] S. Sidhardh, M. C. Ray, Flexomagnetic response of nanostructures, Journal of Applied Physics 124 (2018) 244101.

[20] N. Zhang, Sh. Zheng, D. Chen, Size-dependent static bending of flexomagnetic nanobeams, Journal of Applied Physics 126 (2019) 223901.

[21] M. Malikan, V. A. Eremeyev, Free Vibration of Flexomagnetic Nanostructured Tubes Based on Stress-driven Nonlocal Elasticity. In Analysis of Shells, Plates, and Beams, 1st ed.; Altenbach, H., Chinchaladze, N., Kienzler R., Müller, W. H., Eds.; Springer Nature, Switzerland, 2020; Volume 134, pp. 215-226.

[22] M. Malikan, V. A. Eremeyev, On the geometrically nonlinear vibration of a piezo-flexomagnetic nanotube, Mathematical Methods in the Applied Sciences, (2020). https://doi.org/10.1002/mma.6758

[23] M. Malikan, N. S. Uglov, V. A. Eremeyev, On instabilities and post-buckling of piezomagnetic and flexomagnetic nanostructures, International Journal of Engineering Science 157 (2020) Article no 103395.

[24] M. Malikan, V. A. Eremeyev, K. K. Żur, Effect of Axial Porosities on Flexomagnetic Response of In-Plane Compressed Piezomagnetic Nanobeams, Symmetry 12 (2020) 1935.

[25] M. Malikan, T. Wiczenbach, V. A. Eremeyev, On thermal stability of piezo-flexomagnetic microbeams considering different temperature distributions, Continuum Mechanics and Thermodynamics, (2021). https://doi.org/10.1007/s00161-021-00971-y

[26] M. Malikan, V. A. Eremeyev, Flexomagnetic response of buckled piezomagnetic composite nanoplates, Composite Structures, 267 (2021) 113932.

[27] M. Malikan, R. Dimitri, F. Tornabene, Transient response of oscillated carbon nanotubes with an internal and external damping, Composites Part B: Engineering 158 (2019) 198-205.

[28] M. Malikan, V. B. Nguyen, Buckling analysis of piezo-magnetoelectric nanoplates in hygrothermal environment based on a novel one variable plate theory combining with higher-order nonlocal strain gradient theory, Physica E: Low-dimensional Systems and Nanostructures 102 (2018) 8-28.

[29] M. Malikan, M. Krasheninnikov, V. A. Eremeyev, Torsional stability capacity of a nano-composite shell based on a nonlocal strain gradient shell model under a three-dimensional magnetic field, International Journal of Engineering Science 148 (2020) 103210.

[30] L. Lu, X. Guo, J. Zhao, Size-dependent vibration analysis of nanobeams based on the

nonlocal strain gradient theory, International Journal of Engineering Science 116 (2017) 12–24.

[31] X. Xu, B. Karami, M. Janghorban, On the dynamics of nanoshells, International Journal of Engineering Science 158 (2021) 103431.

[32] X. Xu, B. Karami, D. Shahsavari, Time-dependent behavior of porous curved nanobeam, International Journal of Engineering Science 160 (2021) 103455.

[33] L. Li, Y. Hu, Buckling analysis of size-dependent nonlinear beams based on a nonlocal strain gradient theory, International Journal of Engineering Science 97 (2015) 84-94.

[34] X. Zhu, L. Li, Closed form solution for a nonlocal strain gradient rod in tension, International Journal of Engineering Science 119 (2017) 16-28.

[35] S. Sahmani, B. Safaei, Nonlocal strain gradient nonlinear resonance of bi-directional functionally graded composite micro/nano-beams under periodic soft excitation, Thin-Walled Structures 143 (2019) 106226.

[36] F. Mehralian, Y. Tadi Beni, M. Karimi Zeverdejani, Nonlocal strain gradient theory calibration using molecular dynamics simulation based on small scale vibration of nanotubes, Physica B: Condensed Matter 514 (2017) 61-69.

[37] A. Cemal Eringen, On differential equations of nonlocal elasticity and solutions of screw dislocation and surface waves, Journal of Applied Physics 54 (1983) 4703.

[38] Sh. Dastjerdi, M. Malikan, R. Dimitri, F. Tornabene, Nonlocal elasticity analysis of moderately thick porous functionally graded plates in a hygro-thermal environment, Composite Structures 255 (2021) 112925.

[39] F. Zare Jouneghani, R. Dimitri, F. Tornabene, Structural response of porous FG nanobeams under hygro-thermo-mechanical loadings, Composites Part B: Engineering 152 (2018) 71-78.

[40] R. Gholami, R. Ansari, A unified nonlocal nonlinear higher-order shear deformable plate model for postbuckling analysis of piezoelectric-piezomagnetic rectangular nanoplates with

various edge supports, Composite Structures 166 (2017) 202-218.

[41] R. D. Mindlin, Second gradient of train and surface-tension in linear elasticity, International Journal of Solids and Strucutres 1 (1965) 417-438.

[42] R. D. Mindlin, N. N. Eshel, On first strain-gradient theories in linear elasticity, International Journal of Solids and Strucutres 4 (1968) 109-124.

[43] M. Malikan, Electro-mechanical shear buckling of piezoelectric nanoplate using modified couple stress theory based on simplified first order shear deformation theory, Applied Mathematical Modelling 48 (2017) 196-207.

[44] A. Skrzat, V. A. Eremeyev, On the effective properties of foams in the framework of the couple stress theory, Continuum Mechanics and Thermodynamics 32 (2020) 1779-1801.

[45] M. Akbarzadeh Khorshidi, The material length scale parameter used in couple stress theories is not a material constant, International Journal of Engineering Science 133 (2018) 15-25.

[46] R. Barretta, S. A. Faghidian, R. Luciano, C. M. Medaglia, R. Penna, Free vibrations of FG elastic Timoshenko nano-beams by strain gradient and stress-driven nonlocal models, Composites Part B: Engineering 154 (2018) 20-32.

[47] G.-L. She, H.-B. Liu, B. Karami, Resonance analysis of composite curved microbeams reinforced with graphene nanoplatelets, Thin-Walled Structures 160 (2021) 107407.

[48] M. Malikan, V. A. Eremeyev, On nonlinear bending study of a piezo-flexomagnetic nanobeam based on an analytical-numerical solution, Nanomaterials 10 (2020) 1-22.

[49] R. C. Cammarata, Surface and interface stress effects in thin films, Progress in Surface Science 46 (1994) 1–38.

[50] R. E. Miller and V. B. Shenoy, Size-dependent elastic properties of nanosized structural elements, Nanotechnology 11 (2000) 139–147.

[51] S. Cuenot, C. Fretigny, S. Demoustier-Champagne, and B. Nysten, Surface tension effect on the mechanical properties of nanomaterials measured by atomic forcemicroscopy, Physical Review B 69 (2004) Article ID 165410.

[52] G.-F. Wang and X.-Q. Feng, Effects of surface elasticity and residual surface tension on the natural frequency of microbeams, Applied Physics Letters 90 (2007) Article ID 231904.

[53] J. He and C. M. Lilley, Surface effect on the elastic behavior of static bending nanowires, Nano Letters 8 (2008) 1798–1802.

[54] D.-H. Wang, G.-F. Wang, Surface Effects on the Vibration and Buckling of Double-Nanobeam-Systems, Journal of Nanomaterials, Volume 2011, Article ID 518706, 7 pages.

[55] M. Malikan, V. A. Eremeyev, Post-critical buckling of truncated conical carbon nanotubes considering surface effects embedding in a nonlinear Winkler substrate using the Rayleigh-Ritz method, Materials Research Express 7 (2020) 025005.

[56] R. Gholami, R. Ansari, Nonlinear resonance responses of geometrically imperfect shear deformable nanobeams including surface stress effects, International Journal of Non-Linear Mechanics 97 (2017) 115-125

[57] R. Bellman, B. G Kashef, J. Casti, Differential quadrature: A technique for the rapid solution of nonlinear partial differential equations, Journal of Computational Physics 10 (1972) 40-52.

[58] R. Bellman, J. Casti, Differential quadrature and long-term integration, Journal of Mathematical Analysis and Applications 34 (1971) 235-238.

[59] C. Shu, Differential quadrature and its application in engineering. Berlin: Springer; 2000.

[60] R. Ansari, S. Sahmani, B. Arash, Nonlocal plate model for free vibrations of single-layered graphene sheets, Physics Letters A 375 (2010) 53-62.

[61] L. Behera, S. Chakraverty, Application of Differential Quadrature method in free vibration analysis of nanobeams based on various nonlocal theories, Computers & Mathematics with Applications 69 (2015) 1444-1462.

[62] M. E. Golmakani, J. Rezatalab, Nonlinear bending analysis of orthotropic nanoscale plates in an elastic matrix based on nonlocal continuum mechanics, Composite Structures 111 (2014) 85-97.

[63] M. Malikan, M. Jabbarzadeh, S. Dastjerdi, Non-linear static stability of bi-layer carbon nanosheets resting on an elastic matrix under various types of in-plane shearing loads in thermo-elasticity using nonlocal continuum, Microsystem Technologies 23 (2017) 2973–2991.

[64] M. Malikan, M. N. Sadraee Far, Differential Quadrature Method for Dynamic Buckling of Graphene Sheet Coupled by a Viscoelastic Medium Using Neperian Frequency Based on Nonlocal Elasticity Theory, Journal of Applied and Computational Mechanics 4 (2018) 147-160.

[65] A.J.M. Ferreira, E. Carrera, M. Cinefra, E. Viola, F. Tornabene, N. Fantuzzi, A.M. Zenkour, Analysis of thick isotropic and cross-ply laminated plates by generalized differential quadrature method and a Unified Formulation, Composites Part B: Engineering, 58 (2014) 544-552.

[66] F. Tornabene, N. Fantuzzi, E. Viola, E. Carrera, Static analysis of doubly-curved anisotropic shells and panels using CUF approach, differential geometry and differential quadrature method, Composite Structures, 107 (2014) 675-697.

[67] E. Carrera, A. Pagani, R. Augello, et al. Large deflection and post-buckling of thin-walled structures by finite elements with node-dependent kinematics, Acta Mechanica, 232 (2021) 591–617.

[68] A. Pagani, E. Carrera, Large-deflection and post-buckling analyses of laminated composite beams by Carrera Unified Formulation, Composite Structures, 170 (2017) 40-52.

[69] Z.-l. Lu, P.-z. Gao, R.-x. Ma, J. Xu, Z.-h. Wang, E. V. Rebrov, Structural, magnetic and thermal properties of one-dimensional CoFe2O4 microtubes, Journal of Alloys and Compounds 665 (2016) 428-434.

[70] A. Balsing Rajput, S. Hazra, N. Nath Ghosh, Synthesis and characterisation of pure single-phase CoFe2O4 nanopowder via a simple aqueous solution-based EDTA-precursor route, Journal of Experimental Nanoscience 8 (2013) 629-639.

[71] V. P. Senthil, J. Gajendiran, S. Gokul Raj, T. Shanmugavel, G. Ramesh Kumar, C. Parthasaradhi Reddy, Study of structural and magnetic properties of cobalt ferrite (CoFe2O4) nanostructures, Chemical Physics Letters 695 (2018) 19-23.

[72] L. Li, Y. Hu, L. Ling, Wave propagation in viscoelastic single-walled carbon nanotubes with surface effect under magnetic field based on nonlocal strain gradient theory, Physica E: Low-dimensional Systems and Nanostructures 75 (2016) 118-124.